TISSUE ENGINEERING: Part C
Volume 19, Number 10, 2013
© Mary Ann Liebert, Inc.
DOI: 10.1089/ten.tec.2012.0620

Sustainable Three-Dimensional Tissue Model of Human Adipose Tissue

Evangelia Bellas, BS,[1] Kacey G. Marra, PhD,[2] and David L. Kaplan, PhD[1]

The need for physiologically relevant sustainable human adipose tissue models is crucial for understanding tissue development, disease progression, *in vitro* drug development and soft tissue regeneration. The coculture of adipocytes differentiated from human adipose-derived stem cells, with endothelial cells, on porous silk protein matrices for at least 6 months is reported, while maintaining adipose-like outcomes. Cultures were assessed for structure and morphology (Oil Red O content and CD31 expression), metabolic functions (leptin, glycerol production, gene expression for *GLUT4*, and *PPARγ*) and cell replication (DNA content). The cocultures maintained size and shape over this extended period in static cultures, while increasing in diameter by 12.5% in spinner flask culture. Spinner flask cultures yielded improved adipose tissue outcomes overall, based on structure and function, when compared to the static cultures. This work establishes a tissue model system that can be applied to the development of chronic metabolic dysfunction systems associated with human adipose tissue, such as obesity and diabetes, due to the long term sustainable functions demonstrated here.

Introduction

Adipose tissue engineering has implications for studying adipose tissue development, adipose dysfunction related to diseases, and soft tissue regeneration in a regulated and controlled manner. Adipose tissue is a complex organ with many functions. Once thought of as a static organ for energy storage, adipose tissue has more dynamic roles, including metabolism and endocrine signaling.[1,2] Our understanding of the biology of this tissue is crucial due to links to obesity, type 2 diabetes, cardiovascular risks and associated comorbidities.[3] Currently, adipose tissue biology is mainly studied in the context of cell culture monolayers in *in vitro* culture, or with small animal *in vivo* studies.[4–8] Both methods offer insight to adipose systems, yet neither approximates the complex nature of human adipose tissue.

To address the above needs, suitable cultivation conditions and components must be considered to achieve sustainable long-term structure and function for adipose tissue generated either for *in vitro* or *in vivo* study. Toward this goal, suitable biomaterial scaffolding and cell sources are essential. Silk biomaterials have been used for many years as a suture material, but more recently they have been explored for tissue engineering and regenerative medicine.[9–13] Silk biomaterials can be processed into many formats (gels, tubes, and sponges)[14–16] with a controllable degradation.[17–20] Our group has demonstrated silk biomaterials support adipogenesis both *in vitro* and *in vivo*.[9,13] Often, cells in combination with the biomaterials are needed to establish functional tissues. Human adipose-derived stem cells (ASCs) have been studied over the past decade as an alternative adult stem cell source. They carry fewer ethical concerns and can be obtained through minimally invasive surgery.[21] ASCs are of mesenchymal lineage and therefore are able to differentiate into a variety of cell types including, osteoblasts, adipocytes, myocytes, chondrocytes, and neurons. Recently, they were shown to differentiate into endothelial cells[22,23] and to release many pro-angiogenic factors.[24]

For the study of disease states *in vitro*, the above features can be exploited toward disease-specific tissue models, such as for the study of obesity. The World Health Organization (WHO) broadly defines those individuals who have a body mass index of >30 to be obese (WHO Obesity, 2012).[25] Obesity is a risk factor for other noncommunicable diseases, such as diabetes, cancer, and cardiovascular disease. Obesity affects people of all ages, races, and socioeconomic status. The WHO estimates that about 200 million men and 300 million women were obese in 2008, or about 1/10th of the world adult population. As of 2010, about 43 million children under the age of five were classified as being overweight

[1]Department of Biomedical Engineering, Tufts University, Medford, Massachusetts.
[2]Department of Plastic and Reconstructive Surgery, University of Pittsburgh, Pittsburgh, Pennsylvania.
All work was performed at Tufts University.

(body mass index [BMI]: 25–30), where 35 million lived in developing countries and 8 million in developed countries. Obesity can be attributed to an imbalance of energy in versus energy out. Calorie rich foods and an increasingly sedentary lifestyle are thought to be the biggest contributors to this worldwide epidemic. Many tissues affect whole body metabolism and adipose tissue is a major part of regulating metabolism. Adipocytes take up triglycerides and fatty acids from the blood and store them in their lipid droplet, a process called lipogenesis. The triglycerides are stored in the droplet until needed by other tissues and are subsequently broken down and released for use, in the process of lipolysis. Under overfed conditions, the adipocyte is overloaded with triglycerides and the balance between lipogenesis and lipolysis is offset. Continued accumulation of triglycerides within the adipocyte causes adipocyte hypertrophy, cytoskeletal stress, and macrophage infiltration, eventually leading to the diseased phenotype of obesity.[26,27]

Aside from metabolic functions, adipose tissue also functions as a protective layer for organs and maintains body contours. Soft tissue defects, most often are the result of trauma, congenital defects, or tumor removal. These defects have emotional and social consequences associated with deformity. One method for filling these defects is fat grafting. However, fat grafting, as with other natural and synthetic biomaterial fillers, does not retain volume over time, with 20%–90% of the filler lost over the first few months.[28,29] Therefore, there is a large unmet clinical need for soft tissue fillers that maintain volume. Autografts are a well-studied option for soft tissue reconstruction; however, over half of the grafted material is resorbed within months. In 1951, Peer and Walker reported on the outcome of 28 human fat grafts[30,31] and found that 50% of the transplanted tissue remained after 1 year, whether it was placed near a vascular supply or a like tissue, such as muscle. The adipocytes that did not survive were replaced with fibrotic tissue. More recently, studies have shown that during the process of liposuction and preparation of the lipoaspirate for lipotransfer some of the regenerative aspects are lost.[32,33] For the restoration of traumatic soft tissue defects, the maintenance of tissue size and shape to near normal dimensions for extended time frames is critical to avoid subsequent repeated treatments or surgeries. Current clinical strategies such as free fat transfers and artificial fillers fail to retain volume over time, can require a second surgical site, can result in avascular necrosis, and generally do not regenerate the original tissue.[28,29] The tissue construct must be maintained *in vivo* as the body gradually remodels and regenerates the site into near-normal tissue structure and function.

The goal of this research was to develop a physiologically relevant, long-term model of human adipose tissue that could ultimately serve as (1) a model for studying adipose tissue biology and/or pathologies and (2) as a template for soft tissue regeneration. A slowly degrading yet mechanically sturdy matrix is needed for soft tissue engineering. To address these issues, we developed a three-dimensional (3D) coculture of human ASCs differentiated to adipocytes, cocultured with endothelial cells, on laminin-coated silk protein porous scaffolds. The hypothesis was that a laminin coating would improve initial cellular adhesion while the silk scaffold maintains the structure, architecture, and volume of the soft tissue for at least 6 months *in vitro*.

Materials and Methods

Materials

Bombyx mori silkworm cocoons were supplied by Tajimia Shoji Co. (Yokohama, Japan). All cell culture supplies and collagenase type I were purchased from Invitrogen (Carlsbad, CA) unless otherwise noted. Human recombinant insulin, dexamethasone, pantothenate, biotin, 2,3-thiazolidinediones (TZD), 3-isobutyl-1-methylxanthine (IBMX), bovine serum albumin (BSA), vascular endothelial growth factor (VEGF), and laminin from human placenta were also purchased from Sigma-Aldrich (St. Louis, MO). Primary human adult microvascular endothelial cells and complete endothelial cell media (EGM-2 MV) were purchased from Lonza (Walkersville, MD). Spinner flask units were supplied by Bellco Glass Co. (Vineland, NJ). Histological solvents were purchased from Fisher Scientific (Pittsburgh, PA) and histological reagents were purchased from Sigma-Aldrich. Primary antibody for human CD31 and antibody diluent were purchased from Cell Signaling Technologies (Danvers, MA). The secondary antibody, avidin, biotin complex (ABC) kit, DAB substrate, hematoxylin counterstain, and antigen retrieval solution were purchased from Vector Labs (Burlingame, CA). Enzyme-linked immunosorbent assay (ELISA) kits for human leptin were purchased from R & D Systems (Minneapolis, MN). Glycerol quantification kit was purchased from Sigma-Aldrich. DNA content was assessed using the PicoGreen Assay Kit (Invitrogen). Trizol for RNA isolation was purchased from Invitrogen and RNeasy Mini Kit to purify RNA was purchased from Qiagen (Valencia, CA). All other materials for polymerase chain reaction (PCR), and quantitative PCR, including primers, were purchased from Applied Biosystems (Foster City, CA).

Coated silk scaffold preparation

Silk solution was prepared as published.[18] Briefly, cocoons were chopped and placed in boiling 0.02 M $NaCO_2$ for 30 min to remove sericin, and then washed thrice in ultrapure water. The resulting silk fibroin fibers were left to dry overnight. The dry silk was solubilized in 9.3 M LiBr in 20% w/v at 60°C for 4 h. The silk solution was then dialyzed in ultrapure water in 3500 MWCO membrane for 2 days with a total of six water changes, to remove the LiBr. The 6%–8% w/v aqueous silk solution was lyophilized until dry and resolubilized over 2 days in hexafluoro-2-propanol (HFIP) to generate a 17% w/v silk solution. Salt crystals were sieved to the desired range of 500–600 μm, poured into Teflon-coated Petri dishes and either aqueous silk solution or HFIP-silk solution was added. The Petri dishes were covered and left in a fume hood for 2 days or uncovered to let the HFIP evaporate for 1 day. The dishes were immersed in methanol overnight, left in the fume hood for 1 day for the methanol to evaporate, and then placed in water to leach out the salt particles. The water was changed thrice a day for 2 days. The scaffolds were removed from the Petri dish, cut to the desired dimension, 8 mm diameter × 4 mm height, using a biopsy punch. The scaffolds were left to dry and then autoclaved and kept at 4°C until use. The sterile scaffolds were first rehydrated in phosphate-buffered saline (PBS) for 1 h, and then placed in 10 μg/mL sterile solutions of VEGF, laminin, or VEGF + laminin for 15 min. This coating

procedure was repeated twice and then left overnight to dry. The dry, coated scaffolds were placed into EGM-2 MV media for 1 h before seeding with cells.

ASCs isolation

Subcutaneous adipose tissue was obtained from abdominoplasties under Tufts University IRB (Tufts University IRB Protocol #0906007) from Tufts Medical Center, Department of Plastic Surgery. No identifying information about the patient was obtained, including name, age, BMI, gender, or disease state and therefore only verbal consent was acquired. The specimens were kept at room temperature in saline and used within the same day. The adipose tissue was separated from the skin by blunt dissection and chopped. Chopped adipose tissue was placed into 50 mL conical tubes and minced well with scissors. The tissues were washed in equal volumes warmed PBS, until essentially free of blood. An equal volume of 1 mg/mL collagenase I in 1% BSA in PBS was added to the tissue and placed under gentle agitation at 37°C for 1 h. The tissue samples were centrifuged at 300 *g* for 10 min at room temperature. The supernatant containing the tissue was removed and the pellet resuspended in PBS and centrifuged at the same settings to remove the collagenase solution. The pellet was resuspended in growth media and plated so that 70 g of initial tissue volume was plated per T225 cm^2 tissue culture flask.

Cell culture and 3D static culture

Endothelial cells were cultured and expanded according to the manufacturer's protocol. ASCs were expanded in growth media comprised of Dulbecco's modified Eagle's medium (DMEM)/F12, 10% fetal bovine serum, and 1% penicillin streptomycin fungizone (PSF) until confluence. At 2 days postconfluence, the cells were switched to adipogenic induction media comprised of DMEM/F12, 3% PSF, 1% PSF, 500 μM IBMX, 5 μM TZD, 1 μM dexamethasone, 17 μM pantothenate, 33 μM biotin, and 1 μM insulin until seeded on scaffolds. The endothelial cells were added in 3×20 μL seedings with a total of 800,000 cells/scaffold. The seeded scaffolds were placed in an incubator for 2 h before media was added to the well. The induced ASCs (human adipocytes [hADs]) were added in a similar manner after 1 week, but with 400,000 cells/scaffold. Media was replaced twice per week and maintained in 37°C, humidified incubator.

The experiment timeline is outlined in Figure 1.

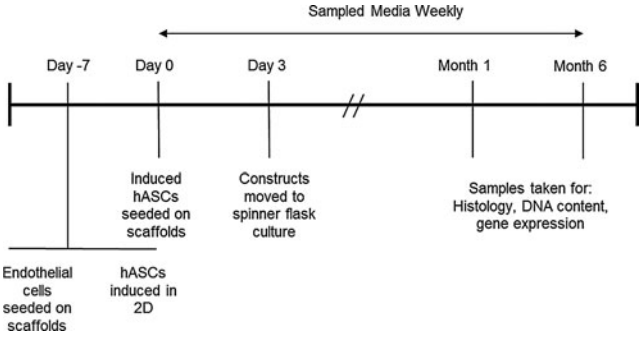

FIG. 1. Experiment timeline for 6-month cultures.

Dynamic (spinner flask) culture

Three days after seeding the induced ASCs the cell-scaffolds were placed on stainless steel wires (2–3 per wire) and hung from the top of 250 mL spinner flasks. A total of 11 seeded scaffolds were contained per spinner flask run at 50 rpm for the duration of the experiment. Media was exchanged twice weekly from the side arms. The scaffolds were transferred to new spinner flasks every 4 weeks.

Media sampling

Media was sampled once per week at the time the constructs were fed. Media samples were stored at −80°C until assayed.

Construct harvest

Constructs were harvested at multiple time points for histology, DNA content, and gene expression. For histological analyses, constructs were cut in half lengthwise, placed in formalin, and used either for cryosectioning or paraffin embedding. For DNA content and gene expression analyses, each construct was placed in a 24-well plate and finely chopped using micro-dissection scissors. Then, 1 mL of Trizol or cell lysis buffer per sample was added and the plates were frozen at −80°C until assayed.

Histology

Constructs were processed according to standard histology protocols. Formalin-fixed samples were put through a series of dehydration solvents and finally paraffin, using an automated tissue processor. Samples were embedded in paraffin, cut in 10 μm sections, and adhered on glass slides. The sections were rehydrated and stained with hematoxylin and eosin (H&E), or underwent antigen retrieval for immunohistochemistry. Nonspecific binding was avoided by incubation with normal blocking serum. After the excess serum was removed, the sections were incubated for 30 min with anti-human mouse CD31 diluted 1:100 in antibody diluent. Sections were washed in PBS and then incubated with a secondary anti-mouse antibody for 30 min. The sections were washed in PBS and then incubated with VECTASTAIN Elite ABC reagent for 30 min, washed in PBS, incubated with ImmPACT DAB enzyme substrate for 5 min, and washed in water. The sections were then counterstained with hematoxylin and mounted.

To evaluate lipid accumulation, the formalin fixed constructs were embedded in optimal cutting temperature medium and frozen. The frozen blocks were cut in 10 μm sections, and then stained with Oil Red O.

Soluble factors

Stored frozen media samples were thawed and immediately assayed according to the manufacturer's protocol for both leptin quantification using an ELISA kit, and glycerol concentration using an enzymatic detection kit.

DNA content

Stored frozen lysates were thawed, centrifuged, and assayed for DNA content using the PicoGreen Assay according to the manufacturer's protocol.

Gene expression

Scaffolds were finely chopped with micro-scissors; RNA was collected from cells using Trizol and stored at −80°C until needed. After thawing, scaffolds were centrifuged at 15,700 *g* for 10 min at 4°C. Supernatants were transferred to new tubes and RNA was isolated using the RNeasy kit according to the manufacturer's protocol. Reverse transcription was performed using high-capacity cDNA reverse transcription kit following the manufacturer's protocol. TaqMan® Gene Expression Assays primers and probes were used for *PPARγ* and *GLUT4* and normalized to the housekeeping gene, *GAPDH*, using the $2^{\Delta\Delta Ct}$ formula.

Statistical analysis

Samples for all quantifiable analyses were $n=4$ with each biological replicate having technical duplicates. *F*-tests were used to determine variance equality and analysis of variances tests were used to compare differences among groups. Histological analyses were performed at $n=3$, with three consecutive sections being taken per staining group; only representative images are shown.

Results

Preliminary experiments to determine scaffold design

Preliminary 6 month 3D coculture experiments were performed to determine which coating(s) yielded the most favorable vascular adipose tissue outcomes in terms of histology, gene expression, and adipokine production, for long-term culture. Three coatings were evaluated and compared to uncoated (control) scaffolds: laminin, VEGF, or laminin, and VEGF. Two scaffold processing windows were examined, those formed from silk processed in aqueous or HFIP (organic solvent) conditions (see Figure 2 in review[34] for an overview of processing windows and porosity).

No significant differences were detected among different coatings or silk types when evaluating gene expression for adipogenic and vasculogenic genes, or leptin (data not shown). Glycerol levels were significantly higher in laminin-coated HFIP scaffold groups (Supplementary Fig. S1; Supplementary Data are available online at www.liebertpub.com/tec). Oil Red O positive staining was seen to be more consistently found throughout the sections in solvent scaffolds while it was found in more localized regions in aqueous scaffolds (Supplementary Fig. S2). In H&E sections, only slight differences in amount of tissue formed were observed between scaffold types, with more tissue formation within solvent scaffolds (Supplementary Fig. S3). When staining for CD31, better organization, that is, in a lumen-like structure, of the remaining endothelial cells was observed on solvent scaffolds (Supplementary Fig. S4). Aqueous scaffolds tended to have disorganized clumps of endothelial cells (Supplementary Fig. S4). From these results, the remainder of the study focused only on two coatings, uncoated and laminin coating on HFIP-silk scaffolds.

Constructs maintained size and shape over six month culture

It was crucial that the scaffold did not degrade in a short time frame and maintained size and shape while the cells had time to form adipose tissue. Constructs were evaluated for changes in size throughout the 6-month experiment (Fig. 2a). The constructs regained their original dimensions after applied pressure was released (Fig. 2b). At 1 month, both static and dynamic cultures averaged 8 mm in diameter. At 6 months, the cultures under static conditions remained at 8 mm, while in dynamic culture the scaffolds increased to 9 mm in diameter (Fig. 2c).

DNA content increases at one month with dynamic culture

DNA content was evaluated to determine relative cell numbers over time (Fig. 2d). In both static and dynamic cultures, DNA content decreased from 1 to 6 months. When comparing static to dynamic cultures at 1 month, DNA content was twofold greater under dynamic conditions. By 6 months, there were no significant differences detected among any of the groups (static, dynamic, uncoated, and coated).

Constructs had improved tissue formation with dynamic culture

Over the 6-month culture period all groups accumulated lipid droplets, a hallmark of maturing adipocytes (Fig. 3). Under static culture conditions cells were found mainly near the periphery of the constructs at both 1 and 6 months. Under dynamic culture conditions (spinner flasks), cells were found consistently throughout the entire construct. Oil Red O positive staining appeared denser at edges of the constructs.

Constructs show continuous lumen formation

Endothelial cells were identified in the cocultures by immunohistochemical staining for CD31. Endothelial cells develop lumen-like structures in all study groups at 6 months (Fig. 4). In static cultures, lumens were found at the periphery (Fig. 4a) while in dynamic cultures, lumen-like structures were found toward the center of the constructs (Fig. 4b). These trends are summarized in the table in Figure 4. Initially, twice as many endothelial cells were seeded as hADs, however, very few remained even after a couple of weeks in culture. Those that did survive were organized into lumen-like structures and were continuous through more than 100 μm of tissue.

Adipogenic gene expression

Gene expression for common adipogenic genes was assessed (Fig. 5). Both *PPARγ* and *GLUT4* were upregulated early in the study when compared to the 1 month uncoated static control, with the greatest level of transcripts for both genes in the static laminin-coated group at 1 month. After 6 months in culture, expression levels for both genes had decreased in all groups; however, dynamic cultures had greater gene expression levels than the static controls. Under dynamic conditions, *PPARγ* levels were maintained, while *GLUT4* expression increased.

Soluble factors increase under dynamic conditions but not significantly with coating or time

Media samples were evaluated for leptin and glycerol production biweekly. Under static conditions, leptin levels at

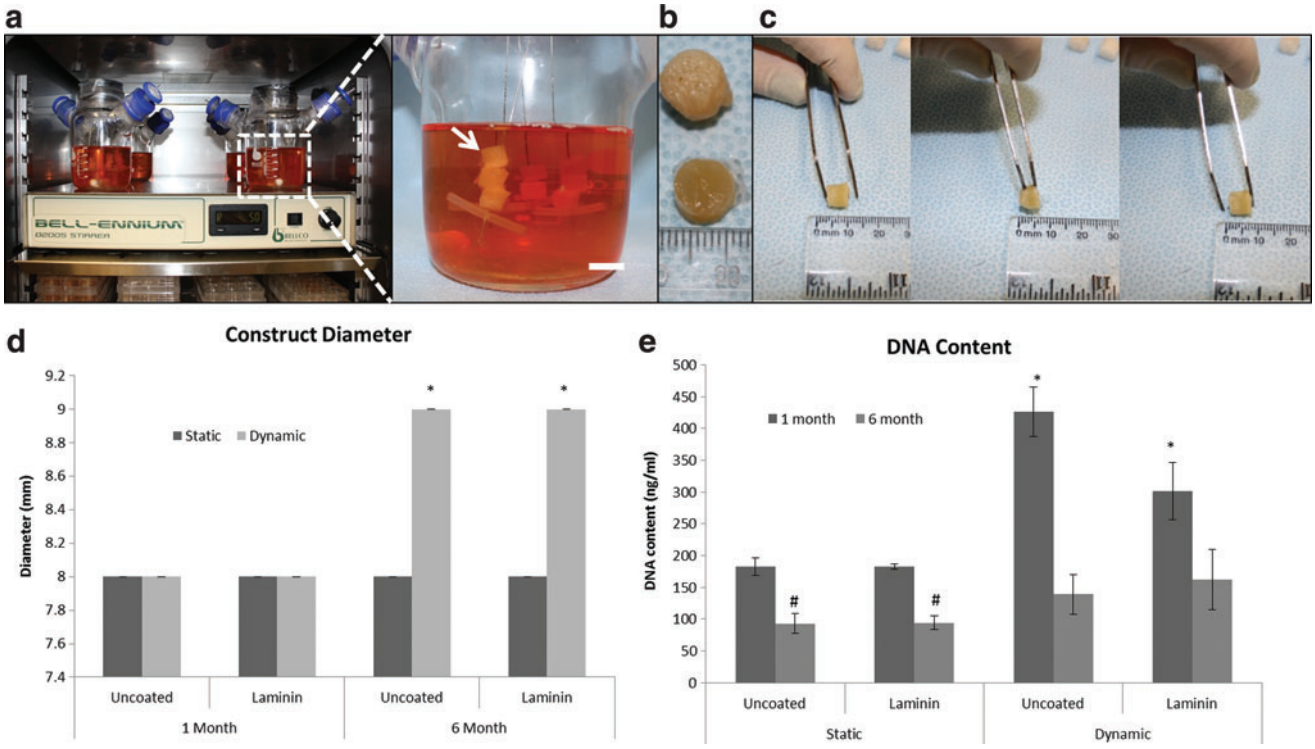

FIG. 2. Constructs maintain size and shape over 6-month culture period. Dynamic culture setup in incubator (left) and zoomed in view of dynamic cultures (right) **(a)**. Macroscopic view of 6-month constructs, bottom row—static cultures, top row—dynamic cultures **(b)**. Constructs return to original dimensions after applied pressure is released **(c)**. Dynamic cultures increased diameter by 1 mm over 6 months of culture—error bars are zero on this scale **(d)**. Diameter change after 6 months in static or dynamic culture conditions. No differences were seen when scaffolds were coated with laminin or with static culture over time. Asterisk indicates significance of $p < 0.0001$. DNA did not increase with long-term culture **(e)**. At 1 month, dynamic cultures had greater DNA content when compared with the controls (static, uncoated group). By 6 months, static cultures had significantly less DNA than controls. At 6 months, dynamic cultures did not have significantly different levels of DNA than the control group. *Indicates significance of $p < 0.001$. #Indicates significance of $p < 0.01$. Color images available online at www.liebertpub.com/tec

1 and 6 months were similar (Fig. 6a). However, at 3 months the levels of leptin were nearly twofold greater than at 1 and 6 months. Under dynamic conditions, leptin levels were also similar to the static group at 1 and 6 months (Fig. 6b). A similar trend was seen where the leptin levels peaked at about 3 months and were nearly 3.5-fold greater than at 1 and 6 months. Glycerol levels did not vary significantly over time under static conditions (Fig. 6c). However, there was a peak glycerol released at 3 months. Under dynamic culture conditions, glycerol levels increased nearly twofold from 1 to 6 months and also peaked at 3 months (Fig. 6d). At 3 months, glycerol levels were more than fourfold higher than at 1 month and twofold greater than at 6 months ($p < 0.001$). No significant differences were found between the uncoated and laminin-coated groups for either leptin or glycerol levels, therefore, only laminin coated groups are shown.

Discussion

The goal of this study was to develop a long-term culture of vascular adipose tissue that could ultimately serve as the basis for studying adipose tissue dysfunction or soft tissue regeneration. In both cases, sustained structure is important. Our preliminary study determined that protein coating (laminin and VEGF) or silk scaffold (aqueous and HFIP) type did not have a significant effect on most adipogenic outcomes (soluble factors and gene expression). Laminin is a basement membrane protein involved in cell adhesion to matrix proteins. VEGF is a potent angiogenic factor. Histological observations demonstrated improved tissue formation and Oil Red O staining on the laminin-coated HFIP-based scaffolds. HFIP-based silk scaffolds have smoother pores when compared with aqueous-based silk scaffolds.[35] These salt-leached porous silk scaffolds, or slight variations of, used in this study have been extensively employed by our group.[9,13,14,18,36–38] These scaffolds have a sponge-like morphology with pores present throughout the scaffold. When salt-leached scaffolds are prepared from different silk solutions, for example, aqueous or solvent, the resulting pore's appearance is altered yielding either "rough" or "smooth" pores.[35,36] We felt it was important to initially compare the two types of pores (rough and smooth) in light of the work linking cellular spreading to stem cell differentiation.[39] Cell density and cytoskeletal forces influence stem cell commitment via the RhoA and ROCK pathways.[39] The HFIP scaffold pores were smoother and had less porosity within individual pore walls than the aqueous-based scaffolds. Therefore, cells were trapped within the pores with little ability to spread and attach. We hypothesize that the smoothness of the pore walls led to increased local cell

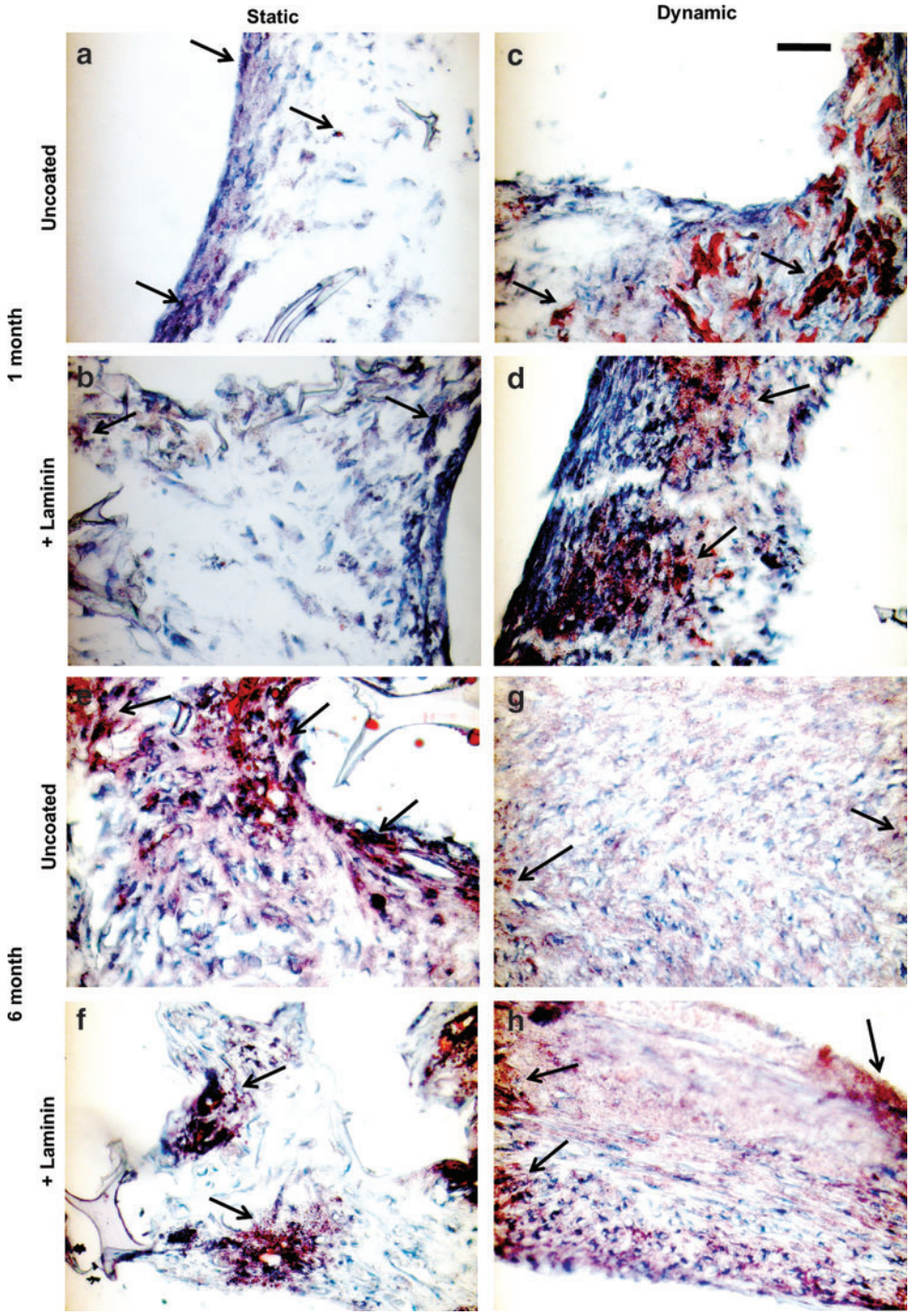

FIG. 3. Dynamic culture improved overall tissue organization. Representative histological images of Oil Red O staining for mature adipocytes after 1 [Top panels, **(a–d)**] and 6 [bottom panels, **(e–h)**] months in static **(a**, **b**, **e**, **f)** and dynamic **(c**, **d**, **g**, **h)** culture conditions. Staining for Oil Red O (arrows) in static cultures was only found at the periphery of the construct, but throughout construct in dynamic cultures. Scale bar: 100 μm. Color images available online at www.liebertpub.com/tec

density and therefore the cells do not experience as much cytoskeletal tension, biasing them toward a more adipogenic program. Alternatively, aqueous-based scaffolds have rougher pore walls so the cells would experience more cytoskeletal tension and would likely be biased toward osteogenic outcomes under basal media conditions. Additionally, laminin improved initial cell adhesion. Given these preliminary outcomes, we chose to continue the studies with laminin-coated HFIP-based silk scaffolds.

Dynamic cultures were explored to improve tissue outcomes as a result of enhanced mass transport and flow to improve the vascular portion. DNA content was not significantly greater in dynamic cultures over time, although an increase in DNA content was seen in the dynamic cultures at 1 month. It is not clear if this was the result of less cell survival in the static group or increased proliferation in the dynamic group. Dynamic cultures contained tissue formation throughout the construct when compared with static groups where cells were mostly found at the periphery. For both static and dynamic cultures to have the same DNA content, the same number of cells must be present but concentrated at the periphery in the static condition. This

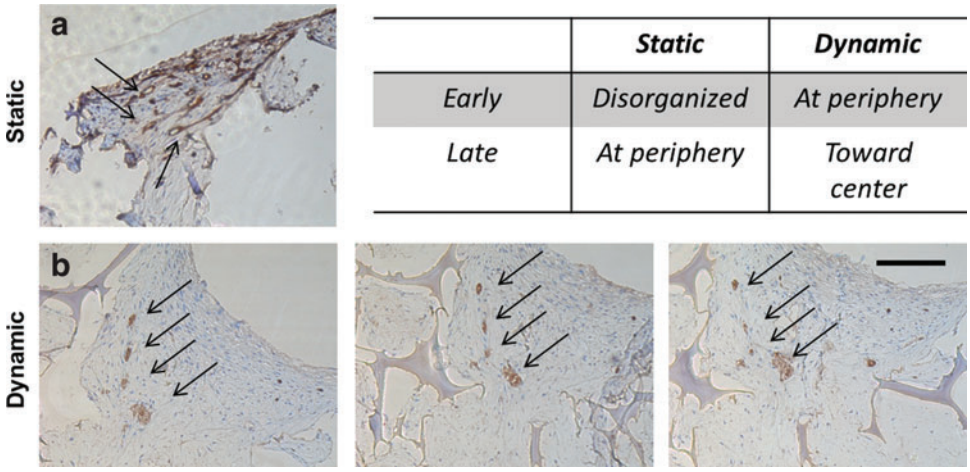

	Static	Dynamic
Early	Disorganized	At periphery
Late	At periphery	Toward center

FIG. 4. Endothelial cells organized into continuous lumen-like structures after 6 months. Representative immunohistological images of CD31 staining (arrows) for lumen formation in laminin-coated scaffold group after 6 months in static **(a)** and dynamic **(b)** culture conditions. Same four lumens are tracked in sections 40 μm apart **(b)**. Table compares endothelial cell organization trend from 1 to 6 months in static and dynamic conditions. Scale bar: 200 μm. Color images available online at www.liebertpub.com/tec

increased concentration of cells could partially explain why the static group had denser Oil Red O staining along the periphery. All groups contained Oil Red O positive cells. In the dynamic groups, most areas of the constructs were positive for Oil Red O staining. Initially, the ratio of hADs to endothelial cells was 1:2, yet not many endothelial cells remained based on CD31 staining. The remaining CD31-positive cells were appropriately organized into lumen-like formations. When we performed our preliminary long-term static studies, CD31 positive cells were found intermittently throughout the construct. These few remaining endothelial cells were not well organized into lumen-like structures over time, hinting that more is needed to sustain these lumen-like structures. Many groups have demonstrated that vascular outcomes are affected by flow.[40–42] We hypothesized flow through the construct (i.e., by spinner flask culture) would help sustain the lumens. After 6 months in culture the best outcome was that only a few lumen-like structures were found remaining, however, this was an improvement from the random clumps of CD31-positive cells seen in static cultures.

In preliminary studies, we found VEGF coating was insufficient to induce robust vasculature. It has been shown that VEGF, although a potent pro-angiogenic factor, may need to be carefully controlled both spatially and temporally.[43] Basic fibroblast growth factor (bFGF) is known to upregulate pro-angiogenic gene expression in endothelial cells.[44] Several groups have included controlled release of bFGF in their adipose tissue-engineered constructs and observed enhanced vascularity, vascular organization, and tissue volume maintenance.[45–47] Although we had bFGF in our cultures, we did not explore how varying bFGF concentration or localization in our cultures may affect vascularity.

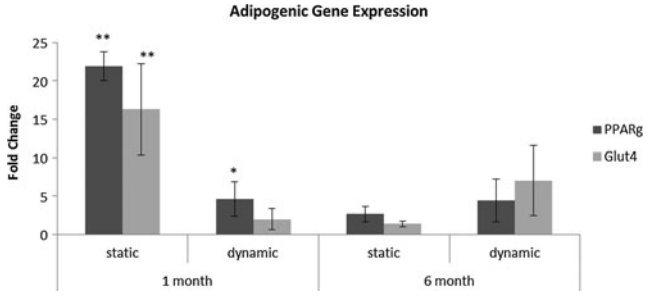

FIG. 5. Adipogenic gene expression decreased over time. Transcript levels for *PPARγ* and *GLUT4* in laminin-coated groups. Levels are relative to 1 month uncoated static control. At 6 months, dynamic cultures had higher transcript levels than static controls. Under dynamic conditions, *PPARγ* levels were maintained, while *GLUT4* expression increased. *Indicates significance $p<0.05$, **Indicates significance $p<0.01$.

To undergo sprouting and vasculogenesis, the endothelial cells need to generate sufficient contractile forces and are better able to do this in softer matrices with fewer binding ligands.[48] It is likely that the silk scaffolds were too stiff to sustain endothelial cells over time. In another study similar results were reported, where independent of seeding ratio of ASCs: endothelial cells or the order of seeding, in cocultures endothelial cell numbers decrease rapidly.[49] The stiffness of silk can be modified by varying processing parameters, however, for long-term culture and slow degradation profile this would have to be tailored carefully. Therefore, increasing the laminin coating or coating with a silk gel may provide a softer substrate for the endothelial cells, while retaining the slow degradation features.

Mechanical and other physical properties were not evaluated in this study. For the purposes of this study, volume stability was critical, because for an obesity model, we need the scaffold to support adipocyte hypertrophy and for a soft tissue implant, a loss of volume is undesirable. This volume stability was achieved by employing solvent-based silk scaffolds, demonstrated to have long degradation rates.[18] Silk scaffolds were previously determined to have a compressive modulus in the tens of kPa,[50–53] just above that of human subcutaneous adipose tissue, which is about 1 kPa.[54] Since no degradation occurred in the time frame studied here, seeding density was relatively low and adipose tissue is dominated by cellular content not matrix such as bone or cartilage, the mechanical properties are assumed to be unaffected and similar to that of the silk scaffold prior to seeding.

Adipogenesis can only occur under control of the transcription factor *PPARγ*,[55] thus serving as an early marker of adipogenesis. *PPARγ* is also continuously expressed through various stages of adipogenesis.[55] The present results showed that expression was highest at 1 month under static

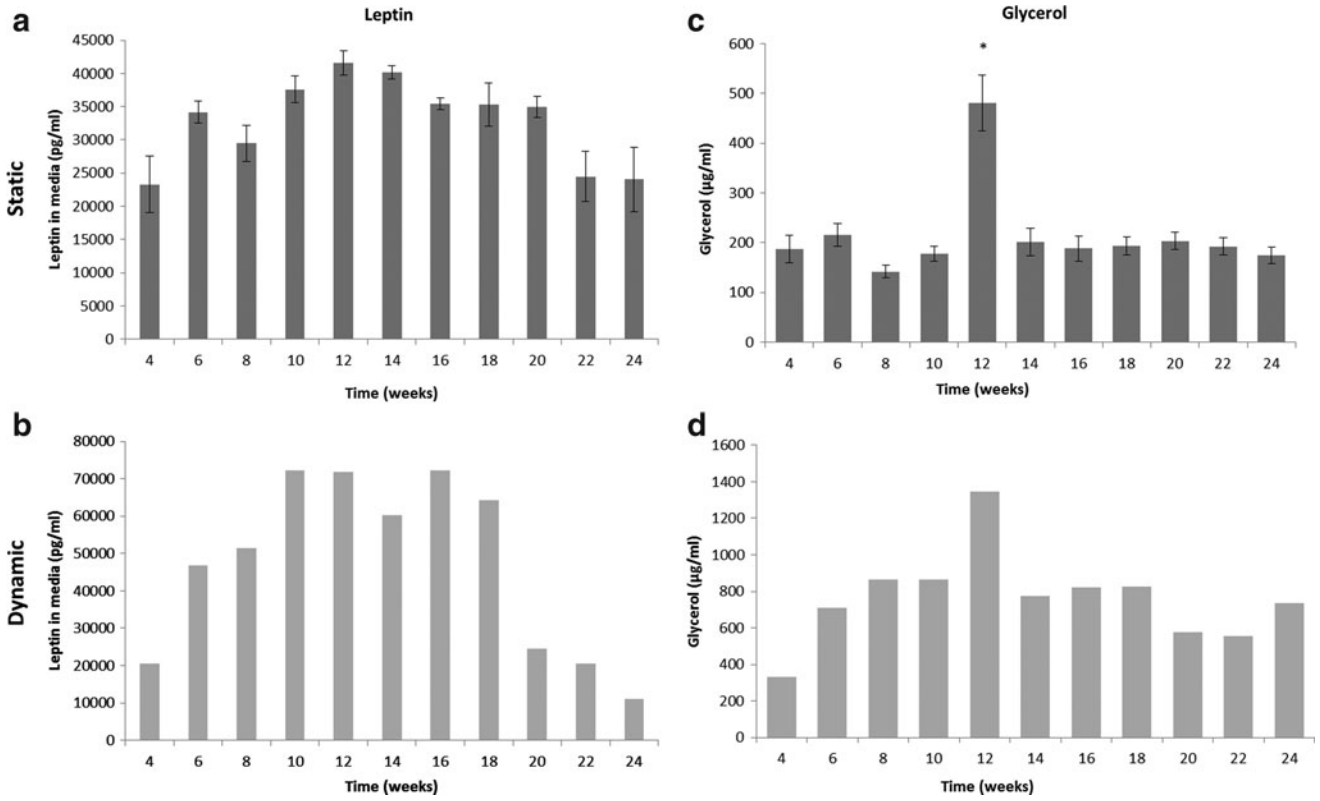

FIG. 6. Leptin **(a, b)** and glycerol **(c, d)** levels increased when cultured under dynamic conditions **(b, d)** when compared with static cultures **(a, c)**. The trends from static cultures were followed under dynamic conditions. No differences were seen when comparing 1 and 6 month cultures; however, the peak level was at 3 months. *Indicates significance level of $p < 0.001$ across time points. *Note:* Error bars are not included in dynamic cultures as all constructs in one group were maintained in the same spinner flask and therefore we cannot decouple each individual construct contribution from the groups.

conditions, and levels did not vary between dynamic groups. We are not aware of a systematic study of the effect of shear forces on adipogenesis. Shear forces may decrease or alter the ability of cells to upregulate *PPARγ* or to undergo adipogenesis at the same rate. *GLUT4* expression did increase, though not significantly, from 1 to 6 months under dynamic conditions. *GLUT4* expression is a late marker of adipogenesis and is partially regulated by the presence of insulin, under dynamic conditions. Thus, under dynamic culture the transport of insulin to the cells may be enhanced.

Leptin is an adipokine released by mature adipocytes that acts on receptors in the brain to signal satiation. Leptin is sensitive to glucocorticoid signaling.[56] The media contained a constant level of dexamethasone, and therefore we expect ongoing secretion of leptin at the time points evaluated. Similarly, glycerol release from lipolysis is also a function of adipocyte maturity. Under the culture conditions in this study, mature adipocytes are likely to undergo lipolysis because insulin (a hormonal mediator of lipolysis) is supplied in the coculture media. Lipolysis is also influenced by glucocorticoids. The media contained constant levels of insulin and dexamethasone; therefore under normal culture conditions we expect the adipocytes to undergo lipolysis. Both leptin and glycerol levels increased with dynamic culture, likely due to increased mass transport. Fluctuations in leptin and glycerol levels at 3 months were found. Since there are no other studies where adipogenesis has been studied *in vitro* for such long-term cultures, it is unclear why there was a significant change at 3 months. Taking the decrease of DNA content into account, it is possible cells had ruptured if they had accumulated too much lipid.

One of the uses for such a model described here was as a model for obesity. Therefore, readouts specific to adipocytes are important. Adipocytes are a central feature of adipose tissue and their ability to accumulate lipids is a defining characteristic of adipogenesis and pathologically, obesity. Adipogenesis can only occur under the control of PPARγ. We demonstrated the accumulation of lipids by Oil Red O staining after *PPARγ* activation. *GLUT4* activation in the presence of insulin is needed for the cell to uptake glucose for its metabolic needs. Leptin and glycerol are markers of metabolic dysfunction used in a clinical setting. As this model is probed under disease conditions, it will be possible to use leptin and glycerol levels to correlate to clinical readouts. In adipose tissue, endothelial cells assist in taking up fatty acids from the blood, while intact vasculature is also needed for nutrient and gas exchange to support the tissue. In future iterations of this model, intact networks of endothelial cells are needed to support these needs to develop a more metabolically functional model of adipose tissue. Whether the goal of this system is to serve as a disease model or for soft tissue regeneration, it is important that tissue outcomes are maintained over long periods of time. Obesity is a chronic disease that evolves as the adipocytes undergo hypertrophy and cytoskeletal stress as the extracellular matrix proteins are broken down and secrete chemokines to

induce inflammation of the tissue. Therefore, many studies to date (i.e., two-dimensional and short-term) do not adequately reflect the complex 3D and chronic nature of adipocyte development and dysfunction. Similarly, the long-term conservation of adipose tissue outcomes is required for successful volume maintenance for soft tissue regeneration.

Conclusions

This work establishes a human 3D tissue model that can ultimately serve as a platform for the development of a metabolic dysfunction model of adipose tissue, and for soft tissue regeneration. The dynamic culture improved adipose tissue formation as seen by Oil Red O positive staining throughout the entire scaffold and improved soluble factor release over static cultures. While this model maintained adipose-like outcomes and functions over a 6-month culture period, the vascular aspects of the system require additional systematic study. The slow degradation rate of silk permitted the sponge to serve as an architectural template for the steady development and maintenance of tissue formation. Thus, the tissue model developed here would be useful in studying chronic states of metabolic disease and long-term effects of potential therapeutics. The robust nature of the silk sponge also makes this system useful for soft tissue regeneration, due to the ease of handling and biocompatibility.

Acknowledgments

The authors would like to thank Jennifer Choi for helpful initial discussions, Jeff Gimble for advice on adipose-derived stem cells and stem cell biology, Dean Glettig for discussions on adipose-derived stem cells, 3D cultures, and assisting with stem cell isolation, and Jonathan Kluge, Pete Galie, and Jordan Miller for advice on article revisions. We would like to thank the NIH P41 (EB002520) Tissue Engineering Resource Center and AFIRM for support.

Disclosure Statement

No competing financial interests exist.

References

1. Tran, T.T., and Kahn, C.R. Transplantation of adipose tissue and stem cells: role in metabolism and disease. Nature Rev Endocrinol **6,** 195, 2010.
2. Ahima, R.S. Adipose tissue as an endocrine organ. Obesity (Silver Spring) **14 Suppl 5,** 242S, 2006.
3. Sethi, J.K., and Vidal-Puig, A.J. Adipose tissue function and plasticity orchestrate nutritional adaptation. J Lipid Res **48,** 1253, 2007.
4. Halvorsen, Y.D., Bond, A., Sen, A., Franklin, D.M., Lea-Currie, Y.R., Sujkowski, D., *et al.* Thiazolidinediones and glucocorticoids synergistically induce differentiation of human adipose tissue stromal cells: biochemical, cellular, and molecular analysis. Metab Clin Exp **50,** 407, 2001.
5. Hemmrich, K., Von Heimburg, D., Cierpka, K., Haydarlioglu, S., and Pallua, N. Optimization of the differentiation of human preadipocytes *in vitro*. Differentiation **73,** 28, 2005.
6. Takahashi, K., Yamaguchi, S., Shimoyama, T., Seki, H., Miyokawa, K., Katsuta, H., *et al.* JNK- and IkappaB-dependent pathways regulate MCP-1 but not adiponectin release from artificially hypertrophied 3T3-L1 adipocytes preloaded with palmitate *in vitro*. Am J Physiol Endocrinol Metab **294,** E898, 2008.
7. Nishimura, S., Manabe, I., Nagasaki, M., Eto, K., Yamashita, H., Ohsugi, M., *et al.* CD8+ effector T cells contribute to macrophage recruitment and adipose tissue inflammation in obesity. Nat Med **15,** 914, 2009.
8. Brommage, R., Desai, U., Revelli, J.-P., Donoviel, D.B., Fontenot, G.K., Dacosta, C.M., *et al.* High-throughput screening of mouse knockout lines identifies true lean and obese phenotypes. Obesity (Silver Spring). **16,** 2362, 2008.
9. Mauney, J.R., Nguyen, T., Gillen, K., Kirker-Head, C., Gimble, J.M., and Kaplan, D.L. Engineering adipose-like tissue *in vitro* and *in vivo* utilizing human bone marrow and adipose-derived mesenchymal stem cells with silk fibroin 3D scaffolds. Biomaterials **28,** 5280, 2007.
10. Kim, H.J., Kim, U.-J., Kim, H.S., Li, C., Wada, M., Leisk, G.G., *et al.* Bone tissue engineering with premineralized silk scaffolds. Bone **42,** 1226, 2008.
11. Lovett, M.L., Cannizzaro, C.M., Vunjak-Novakovic, G., and Kaplan, D.L. Gel spinning of silk tubes for tissue engineering. Biomaterials **29,** 4650, 2008.
12. Subramanian, B., Rudym, D., Cannizzaro, C., Perrone, R., Zhou, J., and Kaplan, D.L. Tissue-engineered three-dimensional *in vitro* models for normal and diseased kidney. Tissue Eng Part A **16,** 2821, 2010.
13. Kang, J.H., Gimble, J.M., and Kaplan, D.L. *In vitro* 3D model for human vascularized adipose tissue. Tissue Eng Part A **15,** 2227, 2009.
14. Altman, G., Diaz, F., Jakuba, C., Calabro, T., and Horan, R. Silk-based biomaterials. Biomaterials **24,** 401, 2003.
15. Vepari, C., and Kaplan, D.L. Silk as a biomaterial. Prog Polym Sci **32(8–9),** 991, 2007.
16. Rockwood, D.N., Preda, R.C., Yücel, T., Wang, X., Lovett, M.L., and Kaplan, D.L. Materials fabrication from *Bombyx mori* silk fibroin. Nat Protoc **6,** 1612, 2011.
17. Numata, K., Cebe, P., and Kaplan, D.L. Mechanism of enzymatic degradation of beta-sheet crystals. Biomaterials **31,** 2926, 2010.
18. Wang, Y., Rudym, D.D., Walsh, A., Abrahamsen, L., Kim, H.J., Kim, H.S., Kirker-head, C., *et al. In vivo* degradation of three-dimensional silk fibroin scaffolds. Biomaterials **29,** 3415, 2008.
19. Pritchard, E.M., Valentin, T., Boison, D., and Kaplan, D.L. Incorporation of proteinase inhibitors into silk-based delivery devices for enhanced control of degradation and drug release. Biomaterials **32,** 909, 2011.
20. Horan, R.L., Antle, K., Collette, A.L., Wang, Y., Huang, J., Moreau, J.E., *et al. In vitro* degradation of silk fibroin. Biomaterials **26,** 3385, 2005.
21. Philips, B.J., Marra, K.G., and Rubin, J.P. Adipose stem cell-based soft tissue regeneration. Expert Opin Biol Ther **12,** 155, 2012.
22. Fischer, L.J., McIlhenny, S., Tulenko, T., Golesorkhi, N., Zhang, P., Larson, R., *et al.* Endothelial differentiation of adipose-derived stem cells: effects of endothelial cell growth supplement and shear force. J Surg Res **152,** 157, 2009.
23. Cao, Y., Sun, Z., Liao, L., Meng, Y., Han, Q., Zhao, C., *et al.* Human adipose tissue-derived stem cells differentiate into endothelial cells *in vitro* and improve postnatal neovascularization *in vivo*. Biochem Biophys Res Commun **332**, 370, 2005.
24. Kilroy, G.E., Foster, S.J., Wu, X., Ruiz, J., Sherwood, S., Heifetz, A., *et al.* Cytokine profile of human adipose-derived stem cells: expression of angiogenic, hematopoietic, and pro-inflammatory factors. J Cell Physiol **212,** 702, 2007.

25. World Health Organization, "Obesity and overweight." www.who.int/mediacentre/factsheets/fs311/en/index.html. Accessed February 27, 2012.
26. Ye, J. Emerging role of adipose tissue hypoxia in obesity and insulin resistance. Int J Obes **33,** 54, 2009.
27. Guilherme, A., Virbasius, J.V., Puri, V., and Czech, M.P. Adipocyte dysfunctions linking obesity to insulin resistance and type 2 diabetes. Nat Rev Mol Cell Biol **9,** 367, 2008.
28. Patrick, C. Tissue engineering strategies for adipose tissue repair. Anat Record **366,** 361, 2001.
29. Gomillion, C.T., and Burg, K.J.L. Stem cells and adipose tissue engineering. Biomaterials **27,** 6052, 2006.
30. Peer, L.A., and Walker, J.C. The behavior of autogenous human tissue grafts; a comparative study. 1. PlastReconstr Surg **7,** 6, 1951.
31. Peer, L.A., and Walker, J.C. The behavior of autogenous human tissue grafts. II. Plas Reconstr Surg **7,** 73, 1951.
32. Yoshimura, K., Sato, K., Aoi, N., Kurita, M., Hirohi, T., and Harii, K. Cell-assisted lipotransfer for cosmetic breast augmentation: supportive use of adipose-derived stem/stromal cells. Aesthetic Plast Surg **32,** 48, 2008.
33. Matsumoto, D., Sato, K., Gonda, K., Takaki, Y., Shigeura, T., Sato, T., *et al.* Cell-assisted lipotransfer: supportive use of human adipose-derived cells for soft tissue augmentation with lipoinjection. Tissue Eng **12,** 3375, 2006.
34. Wang, Y., Kim, H.-J., Vunjak-Novakovic, G., and Kaplan, D.L. Stem cell-based tissue engineering with silk biomaterials. Biomaterials **27,** 6064, 2006.
35. Kim, H.J., Kim, H.S., Matsumoto, A., Chin, I.-J., Jin, H.-J., and Kaplan, D.L. Processing windows for forming silk fibroin biomaterials into a 3D porous matrix. Aust J Chem **58,** 716, 2005.
36. Kim, U.-J., Park, J., Kim, H.J., Wada, M., and Kaplan, D.L. Three-dimensional aqueous-derived biomaterial scaffolds from silk fibroin. Biomaterials **26,** 2775, 2005.
37. Nazarov, R., Jin, H.J., and Kaplan, D.L. Porous 3-D scaffolds from regenerated silk fibroin. Biomacromolecules **5,** 718, 2004.
38. Choi, J.H., Bellas, E., Vunjak-Novakovic, G., and Kaplan, D.L. Adipogenic differentiation of human adipose-derived stem cells on 3D silk scaffolds. In: Gimble, J.M., and Bunnell, B.A., eds. Methods in Molecular Biology. Totowa, NJ: Humana Press, 2011, vol. 702, pp. 319–330.
39. McBeath, R., Pirone, D., and Nelson, C. Cell shape, cytoskeletal tension, and RhoA regulate stem cell lineage commitment. Dev Cell **6,** 483, 2004.
40. Dolan, J.M., Meng, H., Singh, S., Paluch, R., and Kolega, J. High fluid shear stress and spatial shear stress gradients affect endothelial proliferation, survival, and alignment. Ann Biomed Eng **39,** 1620, 2011.
41. Iruela-Arispe, M.L., and Davis, G.E. Cellular and molecular mechanisms of vascular lumen formation. Dev Cell **16,** 222, 2009.
42. Lee, E.J., and Niklason, L.E. A novel flow bioreactor for in vitro microvascularization. Tissue Eng Part C **16,** 1191, 2010.
43. Silva, E.A., and Mooney, D.J. Effects of VEGF temporal and spatial presentation on angiogenesis. Biomaterials **31,** 1235, 2010.
44. Hutton, D.L., Logsdon, E.A., Moore, E.M., Mac Gabhann, F., Gimble, J.M., and Grayson, W.L. Vascular morphogenesis of adipose-derived stem cells is mediated by heterotypic cell-cell interactions. Tissue Eng Part A **18,** 1729, 2012.
45. Stosich, M.S., Moioli, E.K., Wu, J.K., Lee, C.H., Rohde, C., Yoursef, A.M., *et al.* Bioengineering strategies to generate vascularized soft tissue grafts with sustained shape. Methods **47,** 116, 2009.
46. Vashi, A.V., Abberton, K.M., Thomas, G.P., Morrison, W.A., O'Connor, A.J., Cooper-White, J.J., *et al.* Adipose tissue engineering based on the controlled release of fibroblast growth factor-2 in a collagen matrix. Tissue Eng **12,** 3035, 2006.
47. Marra, K.G., Defail, A.J., Clavijo-Alvarez, J.A., Badylak, S.F., Taieb, A., Schipper, B., *et al.* FGF-2 enhances vascularization for adipose tissue engineering. PlastReconstr Surgery **121,** 1153, 2008.
48. Kniazeva, E., and Putnam, A.J. Endothelial cell traction and ECM density influence both capillary morphogenesis and maintenance in 3-D. Am J Physiol Cell Physiol **297,** C179, 2009.
49. Merfeld-Clauss, S., and Gollahalli, N. Adipose tissue progenitor cells directly interact with endothelial cells to induce vascular network formation. Tissue Eng Part A **16,** 2953, 2010.
50. Correia, C., Bhumiratana, S., Yan, L.-P., Oliveira, A.L., Gimble, J.M., Rockwood, D., *et al.* Development of silk-based scaffolds for tissue engineering of bone from human adipose-derived stem cells. Acta Biomater **8,** 2483, 2012.
51. Hofmann, S., Knecht, S., Langer, R., Kaplan, D.L., Vunjak-Novakovic, G., Merkle, H.P., *et al.* Cartilage-like tissue engineering using silk scaffolds and mesenchymal stem cells. Tissue Eng **12,** 2729, 2006.
52. House, M., Sanchez, C.C., Rice, W.L., Socrate, S., and Kaplan, D.L. Cervical tissue engineering using silk scaffolds and human cervical cells. Tissue Eng Part A **16,** 2101, 2010.
53. Tiğli, R.S., Cannizaro, C., Gümüşderelioğlu, M., and Kaplan, D.L. Chondrogenesis in perfusion bioreactors using porous silk scaffolds and hESC-derived MSCs. J Biomed Mater Res Part A **96,** 21, 2011.
54. Patel, P.N., Smith, C.K., and Patrick, C.W. Rheological and recovery properties of poly(ethylene glycol) diacrylate hydrogels and human adipose tissue. J Biomed Mater Res Part A **73,** 313, 2005.
55. Tontonoz, P., and Spiegelman, B.M. Fat and beyond: the diverse biology of PPARgamma. Annu Rev Biochem **77,** 289, 2008.
56. Hwang, C.S., Loftus, T.M., Mandrup, S., and Lane, M.D. Adipocyte differentiation and leptin expression. Annu Rev Cell Dev Biol **13**, 231, 1997.

Address correspondence to:
David L. Kaplan, PhD
Department of Biomedical Engineering
Tufts University
4 Colby St.
Medford, MA 02155

E-mail: david.kaplan@tufts.edu

Received: October 18, 2012
Accepted: January 29, 2013
Online Publication Date: March 8, 2013